# Pilot scale investigation of DBD-Plasma photocatalysis for industrial application in livestock building air: Elimination of chemical pollutants and odors

Wala Abou Saoud, Nacer Belkessa, Ahmed Amine Azzaz, Vincent Rochas, Valerie Mezino, Marie-Amélie Presset, Samuel Lechevin, Anne Genouel, Simon Rouxel, Damien Monsimert, et al.

# Pilot Scale Investigation of DBD-Plasma Photocatalysis for Industrial Application in Livestock Building Air: Elimination of Chemical Pollutants and Odors

Wala ABOU SAOUD[1], Nacer BELKESSA[1], Ahmed Amine AZZAZ[1], Vincent ROCHAS[2], ValerieMEZINO[3], Marie-Amélie PRESSET[2],Samuel LECHEVIN[3],Anne GENOUEL[4],Simon ROUXEL[5], DamienMONSIMERT[5], AbdelkrimBOUZAZA[1], Audrey GLOUX[5], Dominique CANTIN[5], Aymen Amine ASSADI[1,*]

[1]Univ Rennes, ENSCR 11 Allée de Beaulieu, CNRS, ISCR – UMR 6226, F-35708 Rennes, France

[2] Odournet France – Sensenet, 3 allée de Bray 35 510 Cesson-Sevigné – France

[3] SARIA - ALVA – Departement R&D, 3 Rue des Chevaliers 44 412 Rezé- France

[4] SARIA- KERVALIS La Haie Robert, BP 30213 - 35502 Vitre Cedex -France

[5]Asserva SAS, 7 & 9 rue des Gastadours, Maroué, 22403 Lamballe-Armor- France

*Corresponding author: E-mail address: aymen.assadi@ensc-rennes.fr ; Phone : +33 2 23 23 81 52

## Abstract

Photocatalysis and Plasma are widely considered as efficient and eco-friendly methods for the air treatment at domestic and industrial scales. In fact, the respective application of titanium dioxide ($TiO_2$) and Dielectric-Barrier-Discharge(DBD) drew increasing attention in the last decades for their, flexible, non-selective and high efficiencies for the mineralization and the degradation of large selection of molecules. Nevertheless, the application of these techniques in separate conditions might generate undesired by-products that might hinder their treatment efficiencies.In this study, the effect of combining photocatalysis and Dielectric-Barrier-Discharge (DBD)techniques was investigated for the treatment of livestock building air at laboratory and industrial scale. . of Experiments were conducted in separate (i.e.,

Photocatalysis or plasma) and combined (i.e., Photocatalysis and plasma) systems to assess the degradation efficiency of two molecules, namely ($NH_3$) and Propionaldehyde (ProPA) under various operating conditions. Studies onducted on laboratory scale showed a interesting level of treatment when applying either photocatalysis or plasma, with degradation yields reaching 29 and 36% for $NH_3$ and 37 and 42% for ProPA, respectively. These degradation efficiencies were further enhanced when combining the processes, thus reaching 72 and 83% for $NH_3$and ProPA, respectively. Moreover, investigations conducted on the generation of ozone during photocatalysis / Plasma treatment showed a decrease in the $O_3$ concentration when compared to separate Plasma treatment. The photocatalytic degradation of ozone under UV radiation and in presence of $TiO_2$ led to Low concentrations of ozone were detected at joint processas a consequence ofits catalytic decomposition under UV-light into $HO_2^{\circ}$, $OH^{\circ}$,$O_2^{\circ-}$radicals at high humid conditions. The synergetic effect during the pollutant degradation was explained by the association of discharge plasma, presence of $O_3$, UV-light and $TiO_2$..Additionally,The implementation of the photocatalytic-plasma discharge reactor was performed to treat livestock sector air effluent loaded with ammonia.The effect of airflow and relative himidity were assessed. Results showed a significant $NH_3$ removal efficiency in real conditions where it varied between59 and 75% for a flowrate of 2 $m^2/h$ and a relative humidity of 100%. Additonnlay, chemical and olfactometric studies were conducted to assess the performance of cimined sytem with real effllluent of livestock building air.

## Keywords

Photocatalysis, DBD-plasma, livestock building air, Pilot scale investigation, Industrial application.

# 1. INTODUCTION

In the last five decades, the improvement of industrial processes for the fabrication of different types of goods led to a high consumption of first matter and, consequently, to an accelerated tendency of solid, liquid and gaseous wastes generation. In a global context of menacing global warming-related issues, air pollution became a very urgent priority to deal with, particularly by developing reliable, low-cost and sustainable method for the management and treatment of polluted gas streams dispite their chemically complex and heterogeneous contents. Livestock farming is considered as one of the highest contributing economical sectors in the global warming effect [1].In fact, the enteric fermentation, animals respiration and gases released from manure contribute with 56% of the total greenhouse gases (GHG) related to this activity. In fact, polluted air could contain inorganic (ammonia ($NH_3$), hydrogen sulfide ($H_2S$), sulfur dioxide ($SO_2$), nitrogen oxides ($NO_x$)) and/orVolatile Organic Compounds (VOCs; aldehydes, ketones, mercaptans, aromatics etc.) that are commonly released in the atmosphere without a proper treatment [2–4]. Moreover, the presence of these gases even at low concentration inside the closed farming houses could lead to serious health degradation either to human workforce or to the animals.Different techniques were applied for indoor air treatment, such as filtration [5], thermal treatment[6], chemical aerosolization[7], microwave inactivation [8] and physical adsorption [9]. These methods, dispite their confirmed high efficiency for the removal of azerosols, inorganics and volatile compounds, are demanding in terms of energy consumption, installation and maintenance costs which makes their economical and environmental feasability very limited [10].

On the other hand, Advanced Oxidation Processes (AOPs), based on the effect of Ozone ($O_3$) and/or free reactive oxygene species (e.g. $HO_2^{\circ}$; $OH^{\circ}$; $O_2^{\circ-}$), are attracting higher attention as innovative and sustainable technologies for air purification [11,12]. AOPs such as photocatalysis[13,14], non-thermal plasma (NTP)[15]and catalytic ozonation [16] displayed substantial results related to the removal of a variety of chemical pollutants including BTEX (Benzene, Toluene, Ethylbenzene and Xylenes) [17], aldehydes[18], sulfuric [19] and inorganic compounds [20] . Photocatalytic oxidation, based on photo-reactions in the presence of a semiconductor playing the role of a reaction catalyst coupled with the effect of photon source radiation, is known to be a promising technology for its ability to mineralize complex organic pollutants into non-toxic by-products (e.g. $CO_2$ and $H_2O$)[21–28]. Important number of researches dealt with the reactivity of mineral (i.e., $TiO_2$[29], CuO [30], ZnO [31], etc …) and hybrid (Metal doped zeolitic frameworks (ZIF) [32], metal doped organic frameworks (MOF) [33], Immobilized mineral catalysts onto carbon/organic media [34], etc …) catalysts for the treatment of indoor air. Nevertheless, used catalysts showed signs of structural compromise and a decrease in their catalytic activity after an extended operating time and recurrent regeneration cycles. Some studies highlighted the detection of some catalyst-sourced-metals traces in the output of the reactor, thus hindering the ecological advatages of the process.. Another advanced oxidation technology, like non-thermal plasma (NTP) and, especially Dielectric-Barrier-Discharge (DBD), has been applied toward VOCs treatment thanks to its high-effectivenes and non-selective generation of reactivechemical species. for the degradation ofpollutants like toluene/benzene[35,36], trimethylamine [37], ammonia and butyraldehyde [38], hydrogen sulfide [39], sulfur dioxide [40], at room temperature and atmospheric

pressure. Nevertheless, this technology could cause some disadvantages in terms of low $CO_2$ selectivity and undesirableby-products generation (carbon monoxide CO and Ozone ($O_3$)). It is therefore important to develop a cost-effective and highly efficient technology to remove air pollutants. In order to remedy the problems experienced by the separated application of these latter technologies, several studies report that, combining photocatalysis to the plasma discharge provide significant synergyeffects[12,41–44], which could result ina boost of high removal effeciency and a high mineralization selectivety. Recently, photocatalytic-plasma discharge technologies were considered as a suitable technology in terms of gas emissions reduction,low construction and operating costs[45]. Moreover, the ammonia ($NH_3$)/aldehydes removal were studied in some literaturesand a high efficiency was achieved, either at pilot or at industrial scale[38,46–48].

The present work investigates the operating parameters influence, e.g. pollutant (Propionaldehyde, ProPA) initial concentration, air flow rate, relative humidity and input energy. Secondly, a treatment with a photocatalytic and/or discharge plasma reactor were performed at pilot scale (e.g. $NH_3$ and ProPA removal). In addition, mineralization efficiency and plasma by-products inside the pilot reactor are detailed to discuss the ProPA removal behaviors under the optimum operating parameters. Moreover, photocatalytic-plasma discharge technologies were studied, at industrial scale, to control $NH_3$ removal efficiency. The evidence of synergetic effect for industrail application was also investigated. To our knowledge, few studies have been done on the applications of these combined processes on an industrial scale, the conditions of which are very unfavorable in terms of relative humidity, dust and temperature. The fact of confronting this pilot with real conditions makes it possible to emphasize the performance of the process. By-products

identification and Olfactometry tests were also performed with photocatalysis, DBD-plasma and combined process.

# 2. MATERIALS AND METHODS

## 2.1. Materials and chemicals

Ammonia ($NH_3$) was supplied by a gas bottle, and obtained fromAir Liquide Company (Le Boulias, France).Propionaldehyde (ProPA, $CH_3CH_2CHO$, purity = 99%) was purchased from ACROS ORGANICS (Waltham, USA). KI and $Na_2S_2O_3$ solutions were prepared using Ultra-pure-water obtained from a Millipore-Milli-Q system (Burlington, USA). Potassium iodide (KI, purity ≥ 99.5%) was obtained from FLUKA (Bucks, Swizerland). Sodiumthiosulfate ($Na_2S_2O_3$, purity=99%) and hydrochloric acid (HCl) were provided from SIGMA-ALDRICH (Saint-Louis, USA). A commercial catalyst, $TiO_2$Glass Fiber Tissue with 13 $g.m^{-2}$ of colloidal silica, 13 $g.m^{-2}$ of titanium dioxide nanoparticles and inorganic fibers, was used as a photo-catalyst. $TiO_2$-catalyst was graciously provided by Ahlstrom Research and Services (Pont Evêque, France). The catalyst preparation step was already fully described in our previous investigations[49].Physical gas adsorption/desorption analysis reported that the catalyst's specific surface area was about 24 $m^2/g$.

## 2.2. Experimental Setup

The oxidation runs were conducted using the experimental setup shown in **Figure 1**. Atubular reactor formed by two concentric Pyrex tubes (100 cm of length), with a diameter of 58 mm and 76 mm for the inner and the outer tubes, respectively[50][51]. Their wall thickness was about 4 mm. The reactor can be used

asphotocatalysis device by usinganexternal UV lamp (Philips TL 40W/05, 100 cm of length) and/or Dielectric Barrier Dischargeplasma by applying high voltage power. The catalytic component consists of $TiO_2$ deposed onto optical supports, then maintained on the inner reactor wall which can be simultaneously exposed to surface DBD-plasma and UV lamp.Experiments were performed at ambient temperatureand atmospheric pressure Inner temperature and relative humidity were monitored using aTESTO sensor. The inlet flow rate of 2-10 $m^3$/his controlled using a mass flow meter (Bronkhorst In-Flow,Ruurlo, Netherlands). A syringe driver system (Model 100, Kd Scientific, Hollisto, USA) was used for ProPA experiments. An electrical heating band was coiledonthe outside of the injection glass tube to maintain a good evaporation of the pollutant (**Figure 2.a.**). As for ammonia ($NH_3$) gas flow, all experiments were performed using a gas bottle(1000 Mol-ppm) and injected into the reactor and controlled by a flowmeter. Humidity experiments (from 60 to 85± 5%), were performed by bubblingair into a water column. $TiO_2$-catalyst is maintained on the inner reactor wall which can be simultaneously exposed to surface DBD-plasma and UV lamp.

Theplasma reactor was provided with an inner and outer electrode (with aluminum and copper grid, respectively), a signal generator, an amplifier and a digital oscilloscope, all showed in **Figure 1**. To generate DBD-plasma, high voltage power is applied to the reactor. The applied voltage is delivered by a generator (BFi OPTILAS, Lisses, France) as a sinusoidal waveform (at 10 V) andamplified (at 30 kV) using an amplifier(TREK-30 kV model 30/20A, 8 USA)[52][53][48][47]. A digital oscilloscope (Wavesurfer 24 Xs, 200 MHz,Lecroy, Chestnut Ridge, USA) was used to visualize the applied high voltage and the voltage across the capacity.

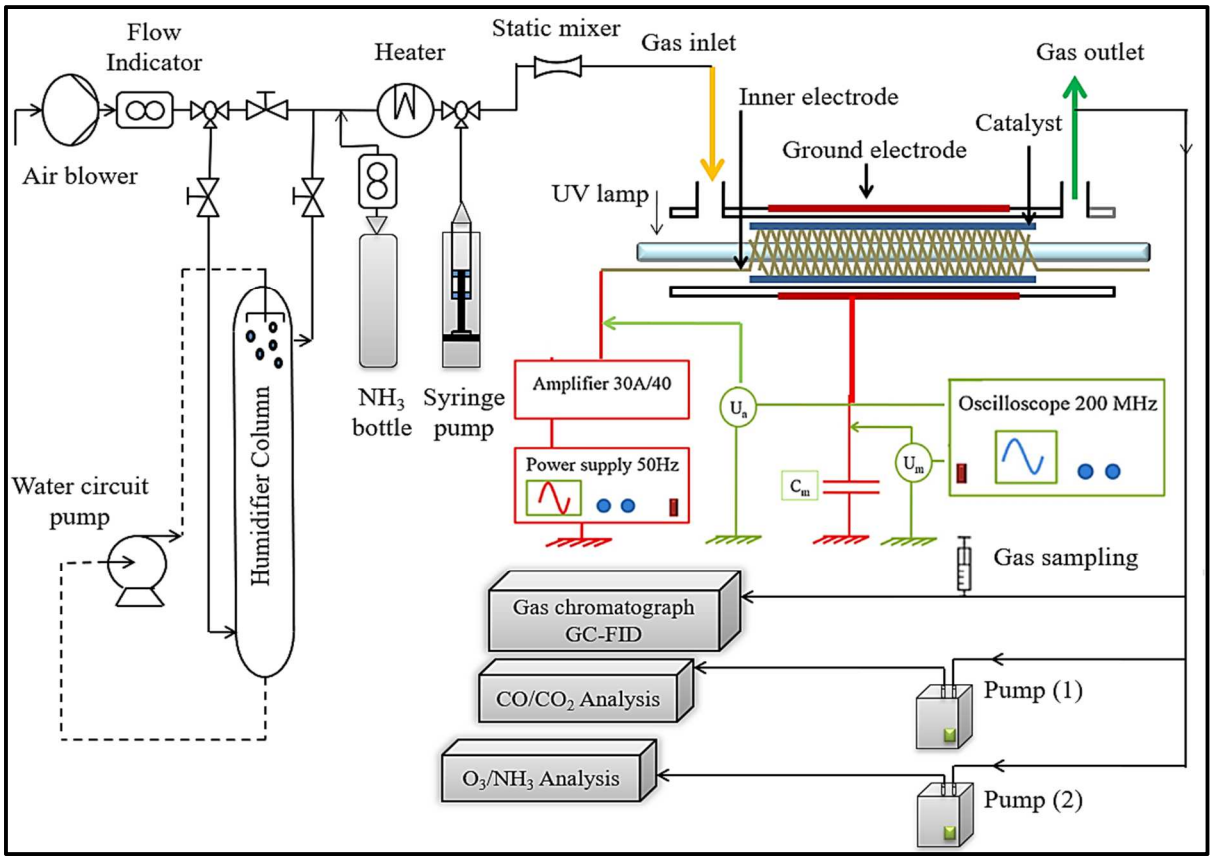


**Figure 1:** General Schematic diagram of the experimental setup.

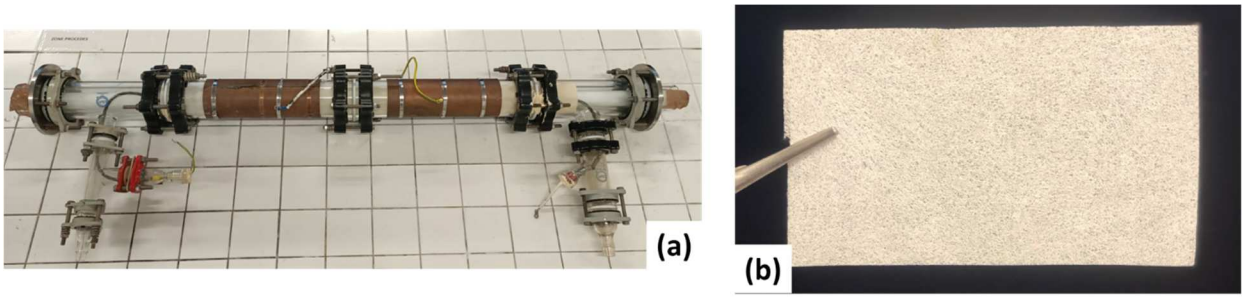


**Figure 2:** Images of (a) the reactor and (b) the used GFT-$TiO_2$ catalyst

## 2.3.Analytical Methods

The ProPA quantification of input/output flow was carried out using Gas Chromatography (Clarus GC-500, Perkin Elmer, Wellesley, USA ). Sample analysis were performed under air hydrogen ($H_2$) and Helium (He) gas flow. Thetemperature

of the injection chamber and the oven were programmed at 250°C and at 40°C for 5min, respectively[50].

The quantification of $NH_3$ was determined through a spectrophotometric method. The ammonia gas phase was directed to a bubbler containing 100 ml of a chloric acid solution (HCl, at 0.1M) by a membrane pump , where it is absorbed as ammonium ion $NH_4$. Nessler's reagent (100 µL) was added to obtain colored solution. $NH_3$ concentration was then determined by measuring light absorbance, at 420 nm, with a spectrophotometer.

CO and $CO_2$ quantification were carried out using a MIR 9000H Fourier Transform Infrared Spectrophotometer (Envea, Poissy, France)Environment SA and a gas analyzer NO/CO ZRE marketed by Fuji Electric (Clermont-Ferrand, France) S.A.S, respectively. The mineralization step was monitored continuously during ProPA degradation. A pumps system (KNF lab, Village-Neuf, France) was used to deliver flow to the $CO/CO_2$ analyzer. The quantification of Ozone was determined using a sodium thiosulfate titration method described thouroughly in our previous paper [38]

The removal efficiency (%) of pollutant (in our case propionaldehyde and ammonia) was determined using Eq. (1):

$$RE\ (\%) = \frac{[Pollutant]_{Inlet} - [Pollutant]_{Outlet}}{[Pollutant]_{inlet}} \times 100 \quad \text{Eq. (1)}$$

where $[pollutant]_{inlet}$ and $[pollutant]_{outlet}$are the initial ($mg/m^3$) and outlet concentration at a given time t, respectively. The specific input energy (SIE; J/L) via plasma system was estimated using Eq. (2):

$$SIE = \frac{3600 \times P}{Q \times 1000} \quad \text{Eq. (2)}$$

where P (W) and Q ($m^3/h$) are the input power adjused by varying applied voltage ($U_a$) and the flow rate, resperctively. The mineralization percentage of CO and $CO_2$ (% SCO and $SCO_2$) was estimated using Eq. (3) and (4):

$$S_{CO}\ (\%) = \frac{[CO_{Outlet}] - [CO_{Inlet}]}{3 \times RE \times [Pollutant]_{Inlet}} \times 10000 \quad \text{Eq. (3)}$$

$$S_{CO_2}\ (\%) = \frac{[CO_{2Outlet}] - [CO_{2Inlet}]}{3 \times RE \times [Pollutant]_{Inlet}} \times 10000 \quad \text{Eq. (4)}$$

### 2.4. By-products identification and Olfactometry tests

Two tests were performed in order to estimate the nature of the inlet and outlet effluent. The first one concerns the odor perceptions (based on specific odorant reference compounds) emitted and formed during process treatement. The second one is an olfactometry test which can evaluate the odour concentration ($uo_E/m^3$) of the effluent. In order to identify pollutants/by-products in the upstream and downstream of the industrial reactor, gas samples were collected on a40Lnalophan bag. The measurements of odor concentration expressed in European Unit Odor($uoE/m^3$) were carried out in accordance with the European standard EN 13725: 2003 "Air quality- determination of odor concentration by dynamic olfactometry", according to the mode of presentation named "forced selection".

## 3. RESULTS AND DISCUSSION

### 3.1. Investigation at pilot scale

#### 3.1.1. Photocatalysis process

- The effect of specific key parameters, namely initial concentration/flow rate and relative humidity, on pollutants removal efficiency was investigated: The target VOC in this study was propionaldehyde (ProPA). The removal efficiency of ProPA using photocatalysis process was studied at an initial concentration of 40-60 mg/$m^3$, an air flow rate of 2-6 $m^3$h and a relative humidity of 60%. The experimental data at various operating conditions were reported in **Figure 3.a.** The result showed that the removal percentage decreased with increasing initial concentration of ProPA and increasing air flow rate. In fact, ProPA removal efficiency (at 40 mg/$m^3$) were 37% at 2 $m^3$/h, 26% at 4 $m^3$/h, and 17% at 6 $m^3$/h. Similarly, at higher initial concentration (60 mg/$m^3$), ProPA removal efficiency decreased to 27% (at 2 $m^3$/h), proving the results reported in our previous study for Chloroform ($CHCl_3$); Glutaraldehyde ($C_5H_8O_2$)[54]; Butane-2,3-dione ($C_4H_6O_2$) and Heptan-2-one ($C_7H_{14}O$) [50] degradation by Cu-Ag/$TiO_2$-based optical fibers at a pilot scale. Similar behavior was observed by Mamaghani et al. [23] and Debono et al. [24] when reported that at higher VOCs concentration, the ratio of active sites/reactive species to VOCs molecules decreases and, consequently, more VOCs remain intact at the end of the process. In addition, a reduction in degradation rate could be remarked since the residence time of VOCs inside the pilot reactor was shortened at high flow rates, which limits the needed reaction time (adsorption + photo-oxidation steps) for the degradation of ProPA [24,38,43,55,56]. As already noted, this study deals with indoor air treatment in the swine rooms and, it is therefore necessary to highlight that air in such structures is usually humid by about 75 to 99.9% of humidity. However, the humidity effect on the ProPA removal was performed by comparing photocatalysis efficiency at various humidity

249 percentages, e. i., 5%, 60% and 85%. As shown in **Figure 3.b,** at a gas flow
250 rate of 2 $m^3$/h and an initial concentration of 40 mg/$m^3$, the ProPA removal
251 percentage under dry air (~ 5%) was 27%, increased to 37% at humidity of ~
252 60% and decreased to 29% at humidity of ~ 85%. ProPA removal efficiency
253 reaches a maximum at humidity of 60%. For the same gas flow, similar
254 behavior was noted when increasing the pollutant's concentration to 60 mg/$m^3$
255 (**Fig 3.b**). Indeed, the ProPA removal efficiency was 21% at dry air (~5%),
256 27% at humid air (~60%) and 20% at high humidity. Therefore, the ProPA
257 removal percentage increased with increase in air humidity and it reached a
258 9% increase at ~60% relative humidity. The performance of ProPA removal
259 can be enhanced with the provision of water vapor molecules decomposition
260 into highly oxidative $OH^{\circ}$-radicals and other reactive species, resulting from the
261 reactions (Eqs. 5-7) [10,57].

262 $$TiO_2 + h\nu \rightarrow e^- + h^+ \quad \text{Eq. (5)}$$

263 $$H_2O + h^+ \rightarrow HO^{\circ} + H^+ \quad \text{Eq. (6)}$$

264 $$VOCs + HO^{\circ} \rightarrow Products + CO_2 + H_2O \quad \text{Eq. (7)}$$

265 Once air humidity reaches an optimum value, antagonist effect is observed
266 described with a decrease in the VOCs removal efficiency. In fact, the exceed in
267 water vapor molecules deactivates of catalyst active sites needed to adsorb/degrade
268 VOCs. Similar results were reported in the literature [21–23,50,58–60].
269

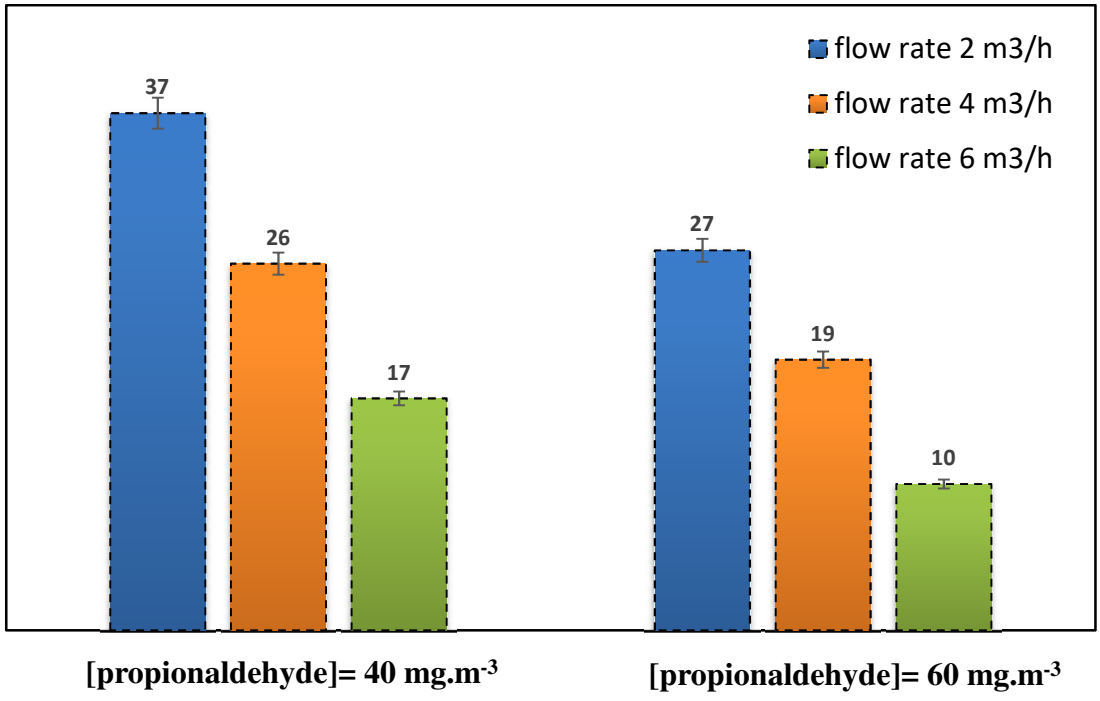


**Figure 3.a.** ProPA removal efficiency obtained by photocatalysis process at differentinlet concentration and flow rate. Experimental conditions:UV intensity20 W/m²;Relative humidity 60%; Temperature 20°C.

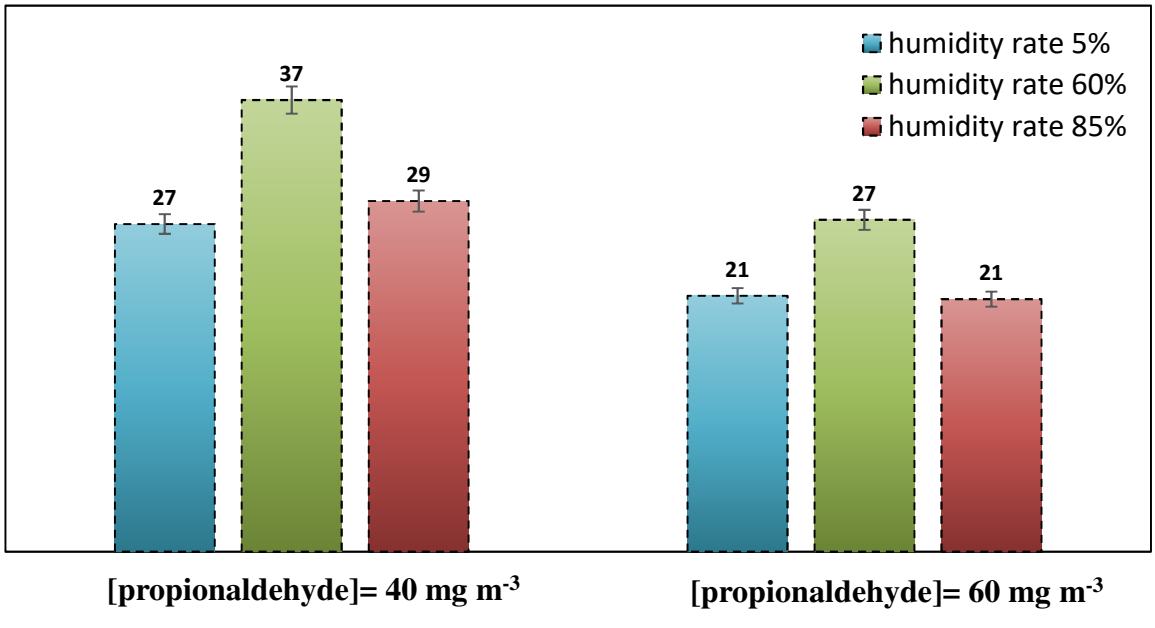

**Figure 3.b.** ProPA removal efficiency obtained at different relative humidity.Experimental conditions: Air flow rate 2 $m^3/h$; UV intensity20 $W/m^2$;Temperature 20°C.

### 3.1.2. Combined DBD plasma-photocatalysis process

#### 3.1.2.1. Removal efficiency

In order to examine the effect of the input energy on the separate removal ofProPA and $NH_3$, DBD plasma/photocatalysis experiments were carried out at different conditions ofspecific energy (6.75 J/L and 11.25 J/L). The $NH_3$/ProPA removal percentagesin DBD plasma alone, photocatalysis alone and combined process at different applied energies are illustrated in **Figure 4**. It is clear that the removal efficiency for both pollutants increased by increasing input energy level. At a gas flowrate of 2 $m^3/h$, an intial concentration of 10-40 $mg/m^3$ and humidity of ~60%, the removal percentage*via* DBD plasma treatment (at 6.75 J/L) increased from 29% and 23% $NH_3$,to 42% and 37%, for ProPA and $NH_3$,respectively (at 11.25 J/L). This behavior is attributed to the synergestic effect of energy input on the accumulation of high-energyelectrons, free radicals, chemicallyactive ions and excited species in the discharge atmosphere [61–63]. Indeed, plasma discharge atmosphere generates more ions (Eqs. 8and 9-11), which leads to the removal efficiency enhancement due to the electron dissociation into reactive species (Eqs. 10 and 11-13) [61,64], as shown in **Figure 4**. It is concluded that the removal efficiency increased with an increasing of input energy because more energy was created in the DBD reactor, and then more reactive species (atomic nitrogen and oxygen) were formed. Reactive species produced in the discharge reactor subsequently reacts with the adsorbed

VOCs, to produce $CO_2$ and $H_2O$ (Mineralization step), as shown in **Figure 5** [61,65,66].

Ionization $e + N_2 \rightarrow 2e + {N_2}^+$ Eq. (8)

$e + O_2 \rightarrow 2e + {O_2}^+$ Eq. (9)

Dissociation $e + N_2 \rightarrow e + 2N^*$ Eq. (10)

$e + O_2 \rightarrow e + 2O^*$ Eq. (11)

As presented in **Figure 4**, removal of $NH_3$/ProPA was better when combining discharge plasma to photocatalysis system. The removal efficiency of $NH_3$, at energy of 11.25 J/L, a gas flow of 2 $m^3$/h and intial concentartion of 10 mg/$m^3$, were 29%, 37% and 73% with photocatalysis, DBD and combined treatment, respectively. As for ProPA, at 11.25 J/L and gas flow of 2 $m^3$/hand intial concentration of 40 mg/$m^3$, experiments show the same degradation trend, and were 36% with photocatalysis, 42% with DBD and 83% with combined treatment. these findings showed that the photocatalytic-DBD reactor provides a better oxidation system for the $NH_3$/ProPA removal at pilot scale, RE ($NH_3$) remains less effectivecompared to Propionaldehyde. In fact, ProPA presents a long molecular chain ($CH_3CH_2CHO$), more easily degradable by DBD plasma/photocatalysis treatment. Associating a photo-catalyst ($TiO_2$) and UV-light in a dielectric barrier discharge reactor presents an excellent source for radicals/excited species. Accordingly, a strong synergy is created between discharge plasma and photocatalysis, which results in a boost of high VOCs efficiency conversion/decomposition and mineralization [44,57,67–69]. It can be deduced that photocatalytic discharge plasma association can increase the

elimination performance of air depollution due to the existence of synergistic effects[70]:

i. Plasma promotes the degradation of photocatalysis by-products by regenerating the catalyst surface. In fact, these molecules remain attached to the $TiO_2$-catalyst surface until their total mineralization. It is believed that plasma discharge enhances the desorption of by-products from the catalyst's functional groups and therefore accelerate their degradation [12,64,71];

ii. Plasma discharge improves $TiO_2$ activation and electron-hole pairs generation, made by ion bombardment [67,72];

iii. At high energy, the discharge accelerates the generation of ionic products, radicals and electrons, which promote the pollutants transfer to the catalyst's surface [12,57,73].

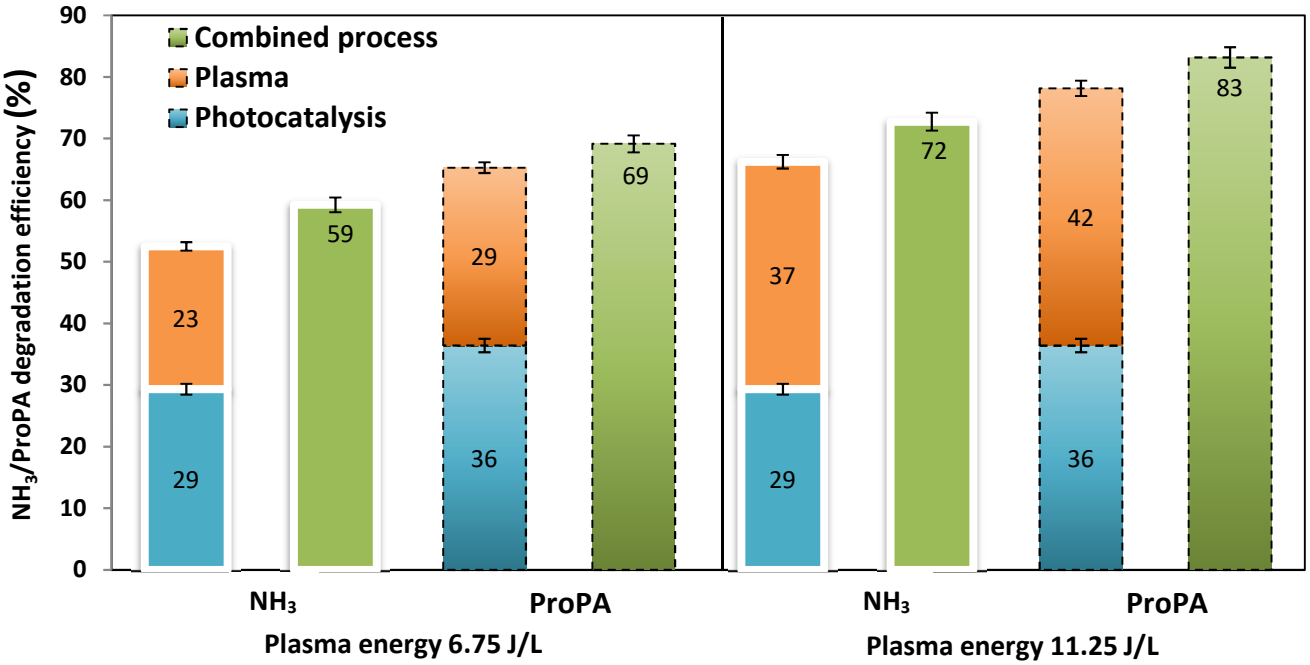


**Figure 4.** $NH_3$/ProPA removal efficiency (%) at differents plasma energy with photocatalysis, DBD plasmaand plasma/photocatalysis combination. Experimental

conditions: initial concentration 10-40mg/$m^3$; Air flow rate 2 $m^3$/h; Relative humidity 60%; Temperature 20°C.

### 3.1.2.2.Mineralization

$CO_2$measurements at the outlet of the plasma/photocatalysis system are taken when the equilibrium state is reached. As shown in **Figure 5**,$CO_2$selectivety increased by combining DBD with photocatalysis. At an air flow of 2 $m^3$/h, an intial concentration of 40 mg/$m^3$ and ~60% of humidity, $CO_2$ selectivety percentage*via* DBD plasma treatment was 39% and increased to 58%at a constant specific energy of11.25 J/L. As for CO selectivety, the experimatal data with photocatalysis, plasma and combined process indicate that CO concentration remained under 11%, as shown in **Figure 5**. In fact , CO decreased from 11 to 6% by combining DBD to photocatalysis, respectively.

As for DBD by-products, Ozone concentration was also monitoried. As presented in **Figure 5**, the concentration zero Ozone decreased from 146.37 to 114.72 ppm when switching from plasma to combined process, respectively. Ozone was valorised by adding photocatalysis to plasma. Thus, reactive oxygene species (e.g. $HO_2^{\circ}$; OH°; $O_2^{\circ-}$) were photo-generated into the $TiO_2$-catalyst surface as a consequence of Ozone decomposition under UV-Light (Eqs. 5, 12-15) [68,74]. Applying an important energy level in presence of UV-light and $TiO_2$-catalyst (e.g. $O_3$ quantity) in the same system showed to be an intersting method way to gain efficiency and process parameters synergies [57,72]. The UV/$TiO_2$/DBD performance was highlighted in terms of ProPA degradationmineralization and DBD by-products.

$$O_3 + OH^{\circ} \rightarrow O_2 + HO_2^{\circ} \quad \text{Eq. (12)}$$

$$O_3 + H^\circ \rightarrow O_2 + OH^\circ \quad \text{Eq. (13)}$$

$$O_3 + e^- \rightarrow O^{\circ -} + O_2 \quad \text{Eq. (14)}$$

$$O_3 + h^+ \rightarrow O^\circ + O_2 \quad \text{Eq. (15)}$$

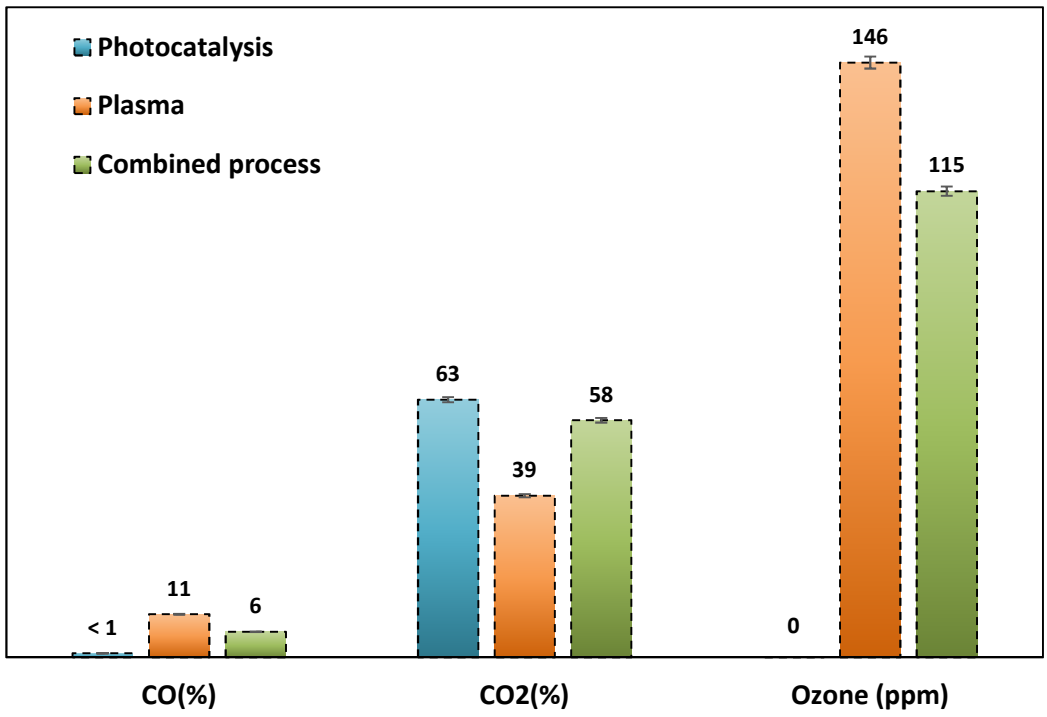


**Figure 5.** Variation of CO/$CO_2$ selectivety (%) and Ozone concentration with photocatalysis, DBD plasma and plasma/photocatalysis combination. Experimental conditions: ProPA concentration 40mg/$m^3$; Air flow rate 2 $m^3$/h; Plasma energy 11.25 J/L;Relative humidity 60%; Temperature 20°C.

### 3.2. Industrial on-site application

The industrial application was performed in collaboration with the IFIP institute (Romillé, France). The prototype was installed and tested to treat air flows generated at a swine experimental station. Ammonia ($NH_3$) was selected as a primary target compound due to building air analysis campaign in the swine rooms. The quantification of $NH_3$gas was continuously monitored on separate days and the

concentration values range between 6 and 25 mg/$m^3$. The exposure limit values of ammonia gas are around 15 mg/$m^3$that can cause a serious risk to human health and to the environment. The industrial study aims to validate the combined process efficiency under real air conditions. The photocatalytic-plasma reactor was installed on IFIP station on July 2021. The tests were performed during the first half of July under 23-25°C of temperature and 75-99.9% of humidity rate. The pilot system that was previously used for ProPA/$NH_3$ degradtion (**Figure 1**) was applied for this study. A modification has been made to the prototype which consists of placing a dust filter at the upstream of the pilot reactor in order to remove any large particles from the ventilation system.

### 3.2.1. Separate degradation process

#### 3.2.1.1. Photocatalysis

The in-field experiments were conducted in real scale scenario and depended dramatically of the punctual swine room conditions, namely temperature, humidity and ammonia concentration in air. Thereby, gas samples were systematically taken in the upstream and downstream of the industrial pilot. Inlet concentrations varied between 14 and 25 mg/$m^3$. The flow rate of the system was 2$m^3$/h and relative humidity was estimated by 86% (higher than lab conditions). **Figure 6** shows the ammonia concentration at the inlet/outlet of the industrial pilot as a function of photocatalysis treatment time. According to results, removal efficiency of ammonia varied over time and depended on itsinitial concentration. The ammonia removal rate fluctuated between 30% and 43% after 7h of irradiationtime.

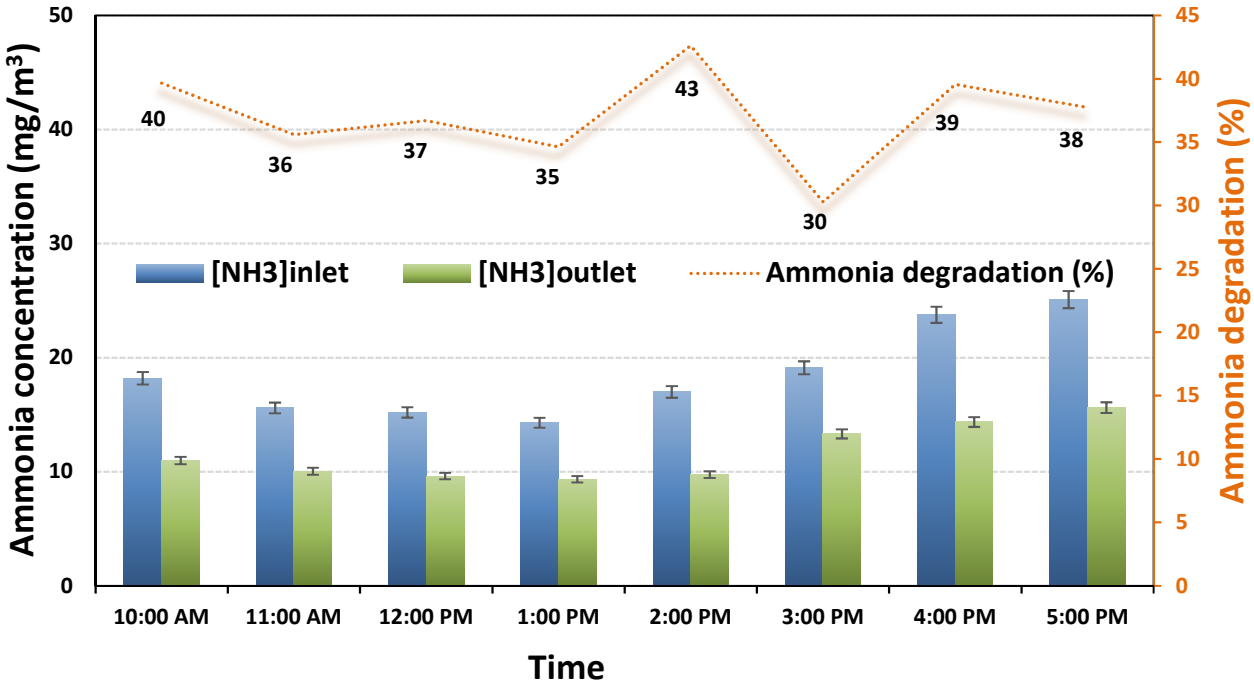


**Figure 6.** Ammonia removal efficiency with photocatalysis process. Experimental conditions: Air flow rate 2 $m^3/h$; Relative humidity 86%; Temperature 23.6°C.

### 3.2.1.2. DBD-plasma

Ammonia treatment was performed using the DBD-plasma process. The flow rate of the system was fixed at 2 $m^3/h$ at a specific energyof 36 J/L, while the humidity percentage was estimated by ~100% (water-saturated air). The variations of humidity percentage and temperature were showed in Table S1. The ammonia concentration at the inlet/outlet of the industrial pilot as a function of plasma treatment time was illustrated in **Figure 7**. Results confirm that $NH_3$removal efficiency was depended intimately on the inlet concentration ([$NH_3$] ~12 and 15 $mg/m^3$). According to **Figure 7**, $NH_3$ removal rate varied between 23% and 34%after 7h of plasma ionization time.

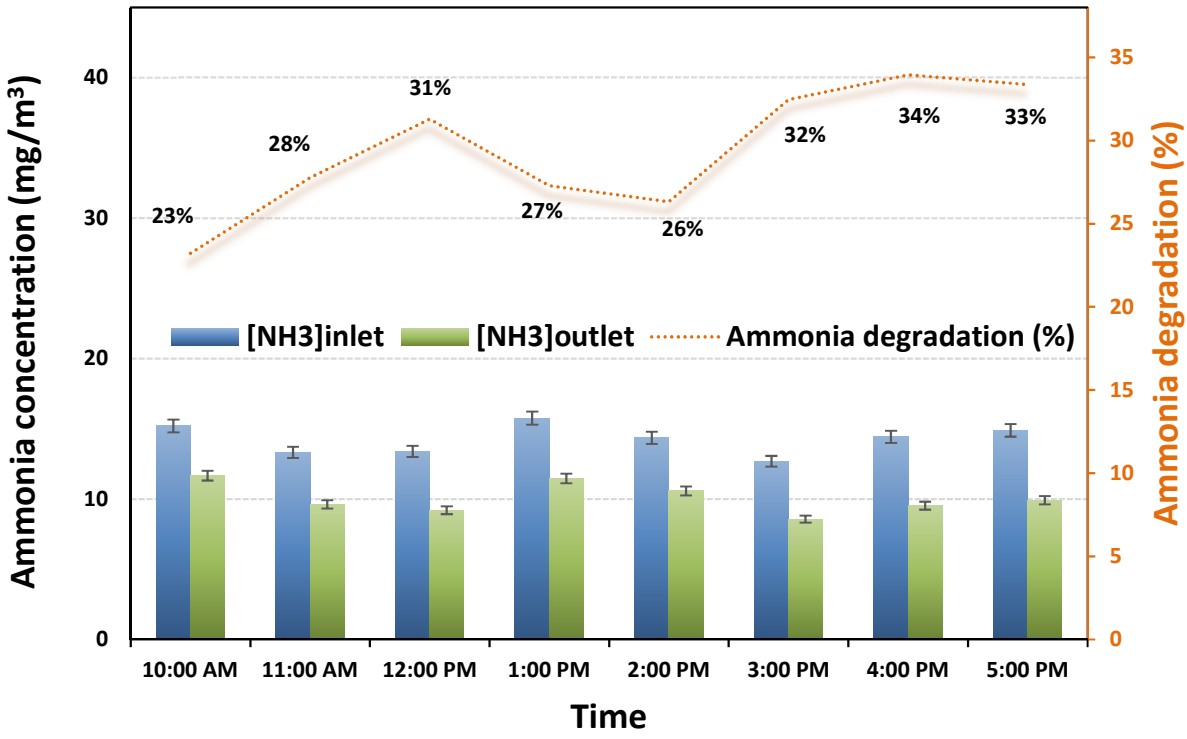


409

410 **Figure 7.**Effect of flow rate on Ammonia removal efficiency. Experimental conditions:;
411 plasma energy 36 J/L; air flow rate 2 $m^3/h$

412 **3.2.2. Plasma and Combined plasma-photocatalysis processes**

413 **3.2.2.1. Removal efficiency**

414 In order to improve the $NH_3$ removal efficiency at high humidity conditions,
415 combined plasma-photocatalysisexperiments were performedunder the same
416 operating conditions, i.e., flow rate ~2 $m^3/h$, specific energy ~ 36 J/L. The variations
417 of humidity percentage and temperature were showed in Table S1. $NH_3$
418 concentrations at the upstream of the pilot reactor were in the range of 13-19 $mg/m^3$.
419 The results of removal efficiency with combined plasma-photocatalysis are illustrated
420 in **Figure 8**. $NH_3$ removal efficiency increased with combined plasma-photocatalysis
421 compared to plasma and photocatalysis when operated separately. The degradation
422 effeciency were estimated by 59-75%, 26-34% and 30-43% for the combined DBD-

photocatalysis, DBD plasma and photocatalysis, respectively, which confirms a synergetic effect of the used techniques at industrial scale.Morever, compared to pilot scale experiments performed at humidity of about 60%, oxidation performance under real100% of humidity was greatly enhanced by coupling processes, which confirms the importance of this promising technology for industrial applications. Furthermore, the high value of humidity does not affect the degradation of $NH_3$ in combined DBD plasma/photocatalysis. This observation corroborates with previous findings[35,38,68,69,72], who confirmed that combined cold plasma to photocatalysis is a great generator of synergism.

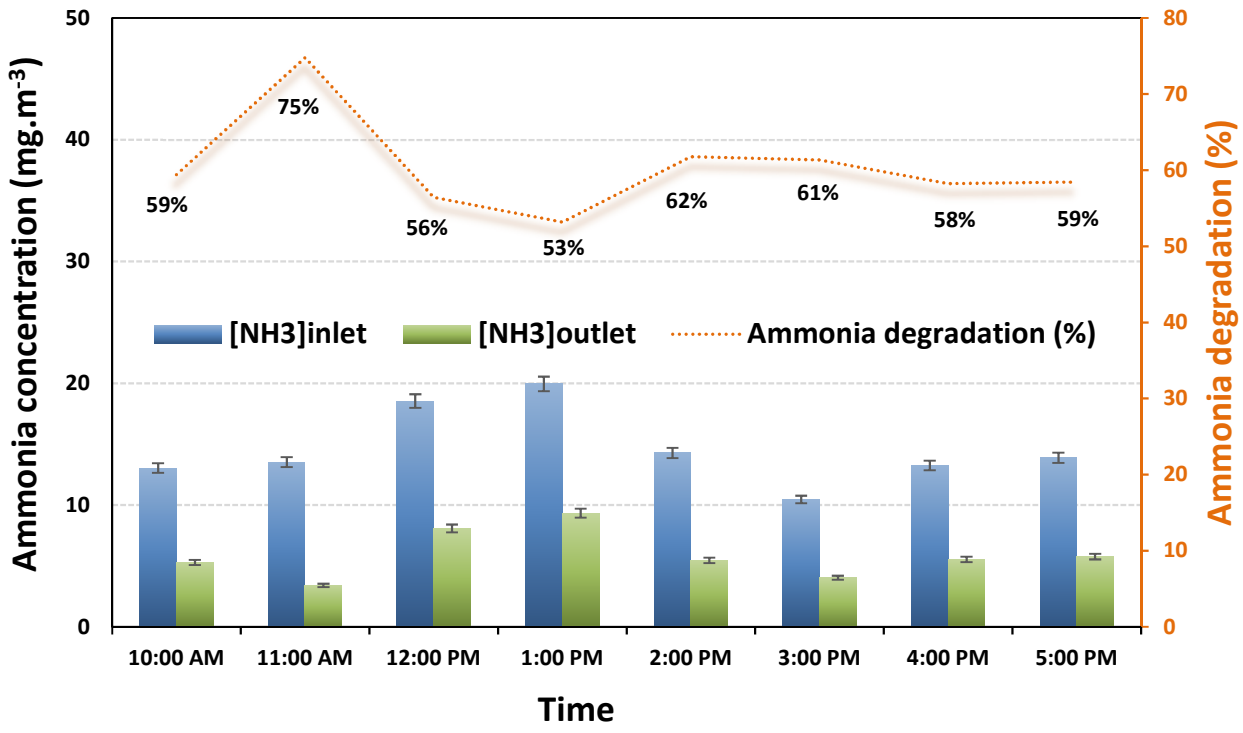


**Figure8.** Effect of flow rate on Ammonia removal efficiency by combined process. Experimental conditions: plasma energy 36 J/L; air flow rate 2 $m^3/h$

In order to examine the effect of the air flow rate on ammonia removal, DBD plasma-photocatalysis experiments were carried out at different air flows (2, 4 and 6

437 $m^3/h$). The variations of humidity percentage and temperature were showed in Table
438 S2. $NH_3$ degradation percentage as a function of the treatment time, at 4 $m^3/h$ and 6
439 $m^3/h$, is illustrated in **Figure 9** and **Figure 10**, respectively. It is clear that the removal
440 efficiency of $NH_3$ decreases with the air stream in the case of 4 $m^3/h$. The
441 degradation efficencies, under DBD plasma-photocatalysis combination, were 59-
442 75% (**Figure 8**) and 27-40% (**Figure 9**) at 2 $m^3/h$and 4 $m^3/h$, respectively. A similar
443 behavior was observed with DBD plasma-photocatalysis system in the case of the
444 experiences at pilot scale. As shown in **Figure 10**, it is worth noting that the inlet
445 concentration was not stable and varied from one experiment to another, as indicated
446 in **Figure 8** (2 $m^3/h$, $[NH_3]$=13-19 $mg/m^3$), **Figure 9**(4 $m^3/h$, $[NH_3]$=11-13 $mg/m^3$) and
447 **Figure 10** (6 $m^3/h$, $[NH_3]$=6-9 $mg/m^3$). The variations of humidity percentage and
448 temperature were showed in Table S3. $NH_3$ concentrations were lower than the ones
449 observed at the previous experiences (6-9 $mg/m^3$ for air flow rate 6 $m^3/h$). In fact, the
450 oxidation efficiencies were around 95-97% for $NH_3$ at 6 $m^3/h$ of air flow, 76% of
451 humidity percentage and 20.8°C of temperature. In this case, the air flow effect was
452 not clear and depended on operating parameters (inlet concentration, relative
453 humidity and temperature) of experiment.

454 As for plasma by-products, the $O_3$ formation as function of plasma and plasma-
455 photocatalysis treatment time for studies at pilot and industrial scale, was illustrated
456 in **Figure 11**. Results showed a decrease in $O_3$ generated quantity by 40% during
457 industrial application (at 100% of humidity) compared to application at pilot scale (at
458 60% of humidity). For the same humidity conditions, Ozone concentration were
459 around 146 and 114 ppmfor DBD plasma and combined process, respectively, while
460 for industrial process, they were estimated by 85 ppm and 68 ppmfor plasma and
461 conmbined process, respectively. Theseresults indicate that the consumption of $O_3$is

462 due to its decomposition by photo-generated radicals, produced at the photocatalyst

463 interface, which contributesto the performance enhancement [38].

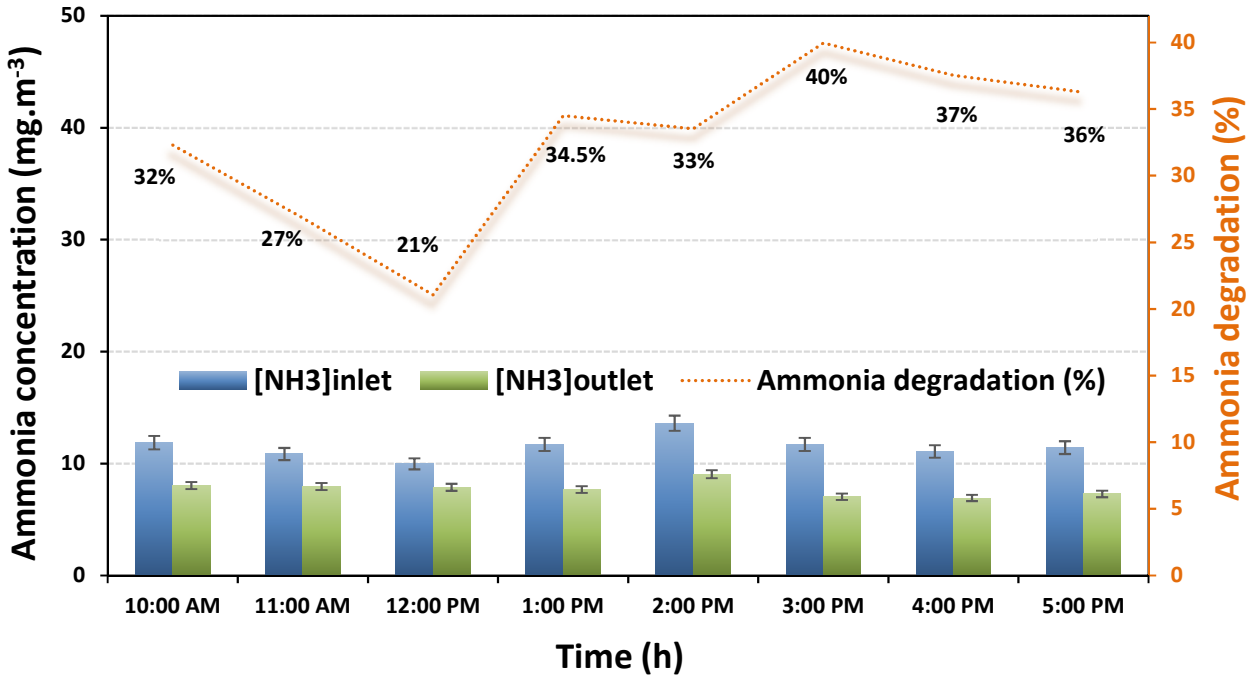


464

465 **Figure 9.** Effect of flow rate on Ammonia removal efficiency. Experimental conditions:

466 plasma energy36 J/L; air flow rate 4 $m^3$/h

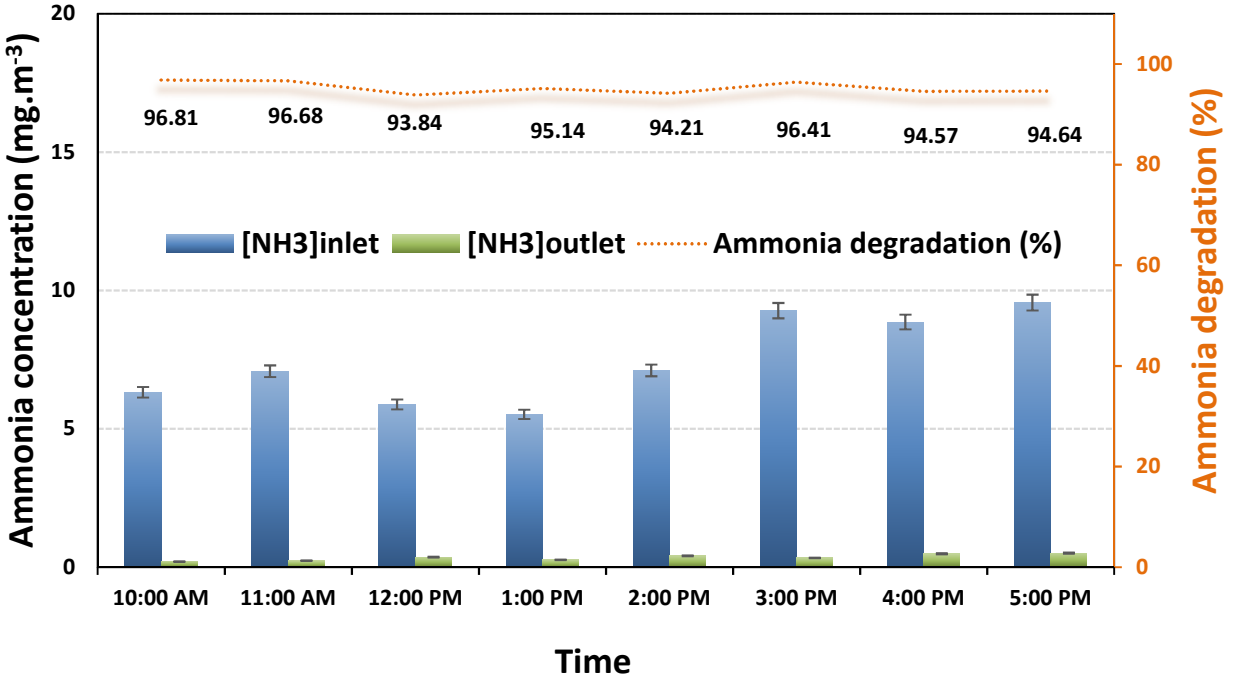


467

**Figure 10.** Effect of flow rate on Ammonia removal efficiency. Experimental conditions: plasma energy 36 J/L; air flow rate 6 $m^3/h$

Online monitoring was carried out with other pollutants such as (Alcohols, aldehydes, aliphatic hydrocarbons, ester, ketones, and sulfur-containing compounds ) which were cocktail with ammonia (pollution feed) (Table S4). The results show that the coupling process has interesting removal rates with organic compounds

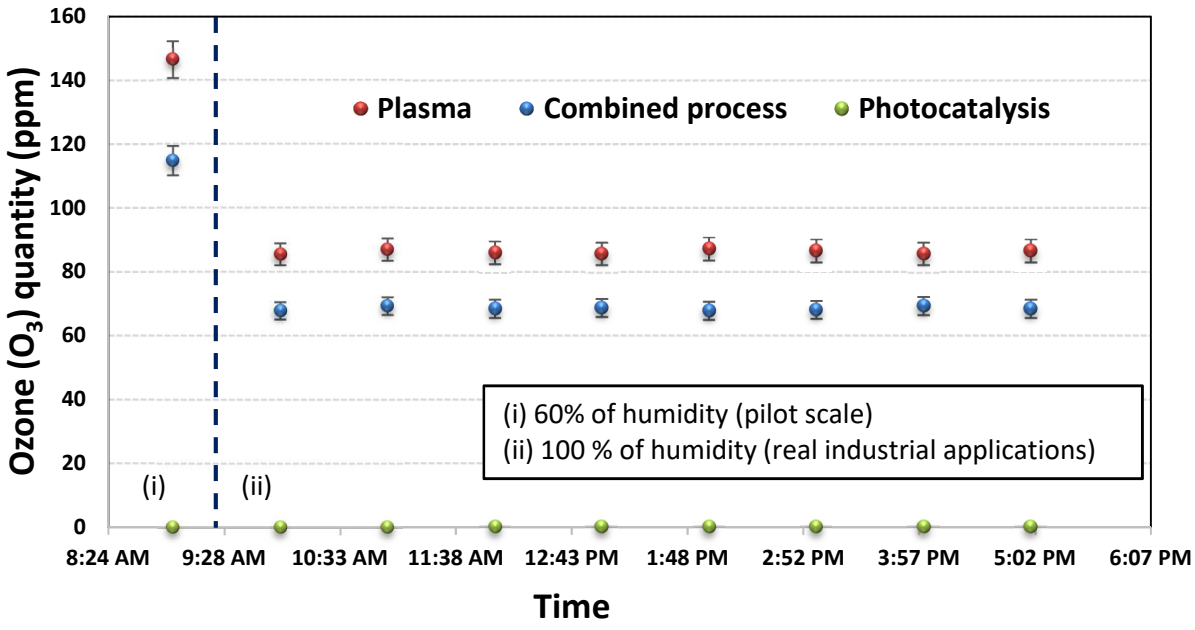


**Figure 11.** $O_3$ quantity as a function of plasma andplasma-photocatalysis treatment time, at pilot (60% of RH) & industrial scale (90-100% of RH). Experimental conditions: $NH_3$concentration 12-25 $mg/m^3$; plasma energy 36 J/L; air flow rate 2 $m^3/h$

### 3.2.2.2.By-products identification and Olfactometry tests

The results for odor perceptions are shown in **Figures 12-14**Ammonia ($NH_3$-pungent/irritant), Hydrogen Sulfide($H_2S$- rotten egg), Butyric Acid ($C_4H_8O_2$- cheese), 3-methylindole ($C_9H_9N$-fecal) were selected as a primary target odor reference compound, present in the inlet gas stream. The detected by-products were

484 essentially: Ozone ($O_3$-fresh/iodized), cis-3-Hexen-1-ol ($C_6H_{12}O$-green grass),
485 Geosmin ($C_{12}H_{22}O$-earthy/musty) and DMDS ($C_2H_6S_2$-rotten vegetable). Globally, the
486 odor intensity remained constant (**Figure . 14**). However, the nature of odor changed
487 due to process treatment. We note that there is no ammonia detected after the
488 oxidation (**Figure 12**). Plasma and combined process also reduced butyric acid and
489 $H_2S$ concentrations. As expected, Ozone is present due to plasma oxidation. The
490 radar chart of odor perceptions (**Figure 13**) shows the evolution of the odor following
491 oxidation process treatment. We note also that the hedonic nature of the odors is
492 increased (**Figure 14**). The value decreased from-2 for the inlet air and reaches -0.5
493 for the coupled process, knowing that -4 refer to very bad odor and +4 very good
494 odors

495

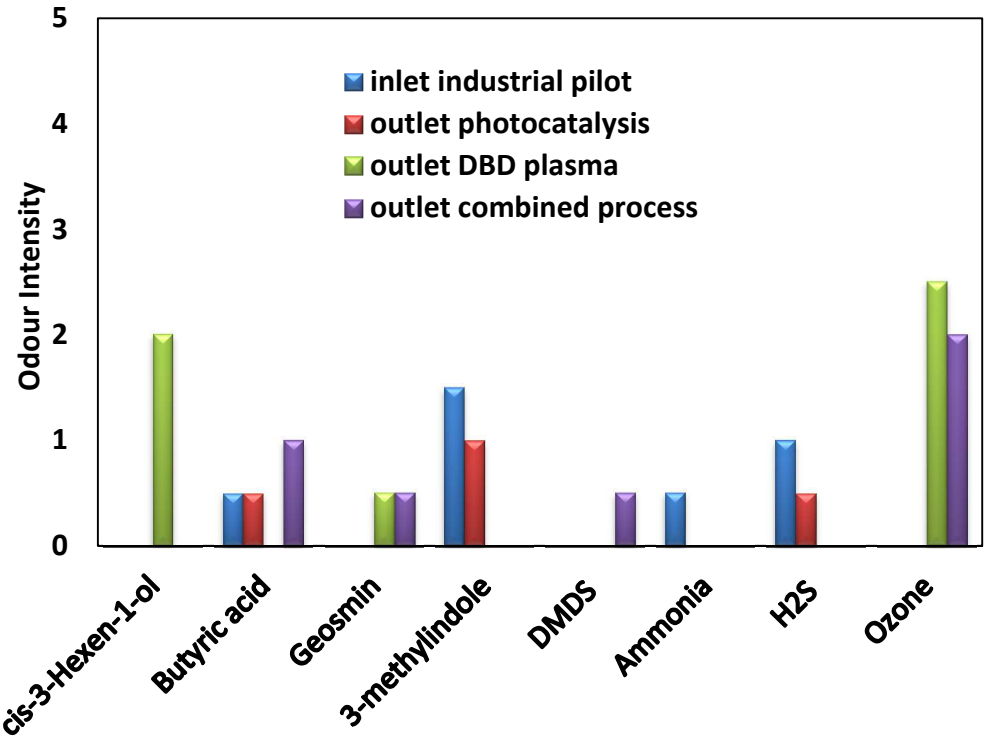


496

**Figure 12.** By-products identification due to photocatalysis,DBD-plasma and combined process. Experimental conditions: $NH_3$concentration 13-19 mg/$m^3$; plasma energy 36 J/L; air flow rate 2 $m^3$/h

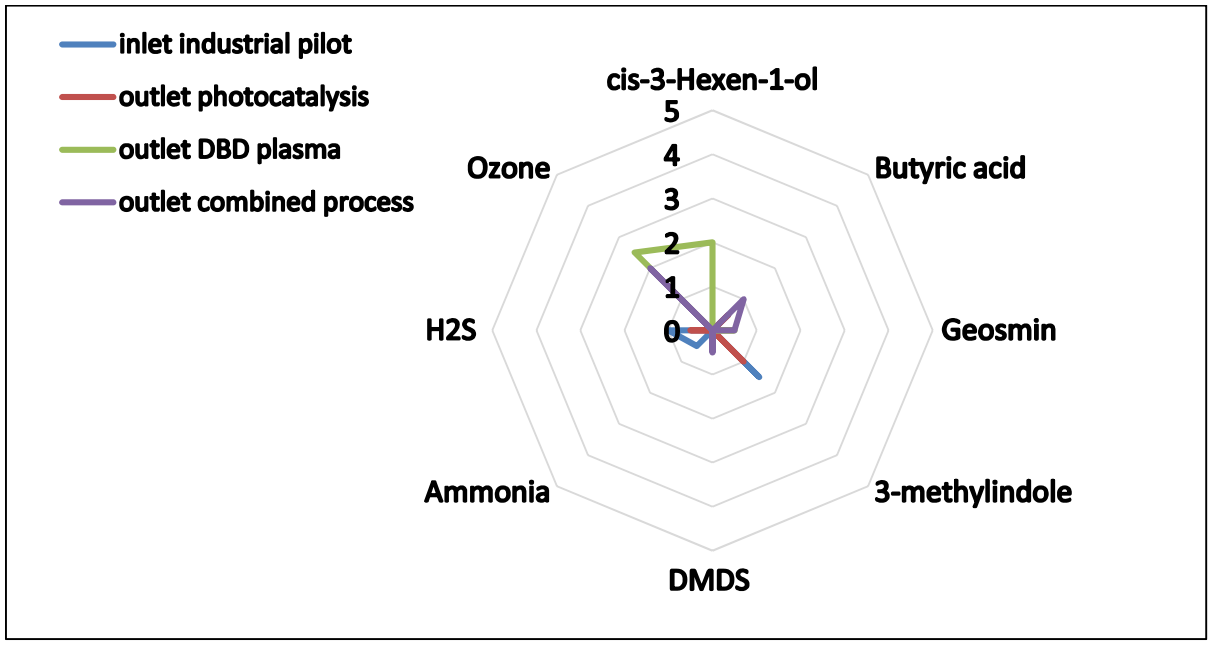


**Figure 13.** Radar Chart of odor perceptions tests with photocatalysis, DBD-plasma and combined process. Experimental conditions: $NH_3$concentration 13-19 mg/$m^3$; plasma energy 36 J/L; air flow rate 2 $m^3$/h

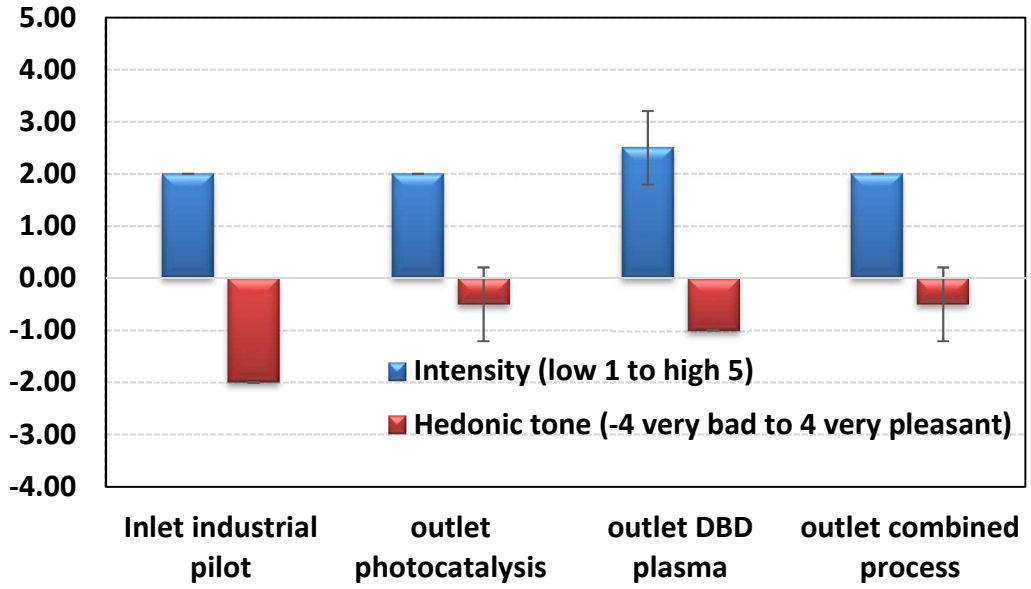

**Figure 14.** Intensity and hedonic tone. Experimental conditions: $NH_3$concentration 13-19 mg/$m^3$; plasma energy 36 J/L; air flow rate 2 $m^3$/h

## 4. Conclusion:

The combination of photocatalysis and plasma was successfully applied for the removal of VOCs/inorganic (ProPA and $NH_3$) pollutants in laboratory and industrial conditions. In the case of laboratory experiments, degradation efficiency was found to increase for high relative humidity (60%), low flowrates (2$m^2$/h) and initial pollutant concentrations (10 mg/$m^3$). The presence of water led to an increase of free radicals' concentrations while lower pollutants concentrations and feed flux ensured more free sites availability and consequently better degradation yields. The combination of plasma and photocatalysis led to a significant decrease in the ozone concentration when compared to the case of sole use of plasma. The presence of $TiO_2$ promoted the degradation of $O_3$ into free radicals that enhanced significantly the degradation performance.

The application of combined DBD-photocatalysis system was investigated (case of ammonia) on industrial emissions from the swine rooms. Results indicate that under important relative humidity varying between 77.9 and 100%, high removal efficiency of 95 to 97% were achieved with less ozone. It is thereby suggested that the use of combined DBD-photocatalysis process can significantly enhance the oxidation performance, increase the VOCs mineralization efficiency and (iii) reduce plasma by-products (CO and $O_3$).

**5. Acknowledgment**

This study was financially supported byregion of Brittany-France and European Regional Development Fund-(Elev'Air project_Ref EU001000).

# References

[1] V. Sejian, J. Gaughan, L. Baumgard, C. Prasad, Climate change impact on livestock: Adaptation and mitigation, Climate Change Impact on Livestock: Adaptation and Mitigation. (2015) 1–532. https://doi.org/10.1007/978-81-322-2265-1.

[2] France. Agence de l'environnement et de la maîtrise de l'énergie, Pollutions olfactives : Origine - Législation - Analyse - Traitement, 2008.

[3] S.N. Behera, M. Sharma, V.P. Aneja, R. Balasubramanian, Ammonia in the atmosphere: A review on emission sources, atmospheric chemistry and deposition on terrestrial bodies, Environmental Science and Pollution Research. 20 (2013) 8092–8131. https://doi.org/10.1007/s11356-013-2051-9.

[4] M. Schiavon, V. Torretta, A. Casazza, M. Ragazzi, Non-thermal Plasma as an Innovative Option for the Abatement of Volatile Organic Compounds: a Review, Water Air Soil Pollut. 228 (2017). https://doi.org/10.1007/s11270-017-3574-3.

[5] A.A. Azzaz, A.A. Assadi, A.A. Assadi, Integration of nondestructive processes: adsorption/uptake/absorption, in: Hybrid and Combined Processes for Air Pollution Control, Elsevier, 2022: pp. 345–356. https://doi.org/10.1016/B978-0-323-88449-5.00015-2.

[6] J. Yu, J. Yang, W. Yan, Thermodynamic simulation and experiment research of the solar air evaporating separation system for saline wastewater treatment with thermal collector–evaporator integrated unit, Energy Reports. 8 (2022) 6707–6728. https://doi.org/10.1016/J.EGYR.2022.05.025.

[7] Y.H. Lu, H. Wu, H.H. Zhang, W.S. Li, A.C.K. Lai, Synergistic disinfection of aerosolized bacteria and bacteriophage by far-UVC (222-nm) and negative air ions, J Hazard Mater. 441 (2023) 129876. https://doi.org/10.1016/J.JHAZMAT.2022.129876.

[8] P. Sharma, H.W. Xiao, Q. Zhang, P.P. Sutar, Intermittent high-power short-time microwave-vacuum treatment combined with steam impingement for effective microbial decontamination of black pepper (Piper nigrum), J Food Eng. 343 (2023) 111373. https://doi.org/10.1016/J.JFOODENG.2022.111373.

[9] Y. Wang, J.T. Anyanwu, Z. Hu, R.T. Yang, Significantly enhancing CO2 adsorption on Amine-Grafted SBA-15 by boron doping and acid treatment for direct air capture, Sep Purif Technol. 309 (2023) 123030. https://doi.org/10.1016/J.SEPPUR.2022.123030.

[10] T. Zadi, M. Azizi, N. Nasrallah, A. Bouzaza, R. Maachi, D. Wolbert, S. Rtimi, A.A. Assadi, Indoor air treatment of refrigerated food chambers with synergetic association

between cold plasma and photocatalysis: Process performance and photocatalytic poisoning, Chemical Engineering Journal. 382 (2020) 122951. https://doi.org/10.1016/J.CEJ.2019.122951.

[11] B.M. da Costa Filho, V.J.P. Vilar, Strategies for the intensification of photocatalytic oxidation processes towards air streams decontamination: A review, Chemical Engineering Journal. 391 (2020) 123531. https://doi.org/10.1016/j.cej.2019.123531.

[12] M. Qu, Z. Cheng, Z. Sun, D. Chen, J. Yu, J. Chen, Non-thermal plasma coupled with catalysis for VOCs abatement: A review, Process Safety and Environmental Protection. 153 (2021) 139–158. https://doi.org/10.1016/j.psep.2021.06.028.

[13] C. Li, L. He, X. Yao, Z. Yao, Recent advances in the chemical oxidation of gaseous volatile organic compounds (VOCs) in liquid phase, Chemosphere. 295 (2022) 133868. https://doi.org/10.1016/J.CHEMOSPHERE.2022.133868.

[14] R. Fiorenza, R.A. Farina, E.M. Malannata, F. Lo Presti, S.A. Balsamo, VOCs Photothermo-Catalytic Removal on MnOx-ZrO2 Catalysts, Catalysts. 12 (2022) 85. https://doi.org/10.3390/CATAL12010085/S1.

[15] Z. Jia, M. Ben Amar, D. Yang, O. Brinza, A. Kanaev, X. Duten, A. Vega-González, Plasma catalysis application of gold nanoparticles for acetaldehyde decomposition, Chemical Engineering Journal. 347 (2018) 913–922. https://doi.org/10.1016/j.cej.2018.04.106.

[16] B.M. da Costa Filho, G. V. Silva, R.A.R. Boaventura, M.M. Dias, J.C.B. Lopes, V.J.P. Vilar, Ozonation and ozone-enhanced photocatalysis for VOC removal from air streams: Process optimization, synergy and mechanism assessment, Science of the Total Environment. 687 (2019) 1357–1368. https://doi.org/10.1016/j.scitotenv.2019.05.365.

[17] C.A. Korologos, M.D. Nikolaki, C.N. Zerva, C.J. Philippopoulos, S.G. Poulopoulos, Photocatalytic oxidation of benzene, toluene, ethylbenzene and m-xylene in the gas-phase over TiO 2-based catalysts, J Photochem Photobiol A Chem. 244 (2012) 24–31. https://doi.org/10.1016/j.jphotochem.2012.06.016.

[18] A.A. Assadi, A. Bouzaza, D. Wolbert, Photocatalytic oxidation of trimethylamine and isovaleraldehyde in an annular reactor: Influence of the mass transfer and the relative humidity, J Photochem Photobiol A Chem. 236 (2012) 61–69. https://doi.org/10.1016/j.jphotochem.2012.03.020.

[19] Y.H. Lin, H.T. Hsueh, C.W. Chang, H. Chu, The visible light-driven photodegradation of dimethyl sulfide on S-doped TiO2: Characterization, kinetics, and reaction pathways, Appl Catal B. 199 (2016) 1–10. https://doi.org/10.1016/j.apcatb.2016.06.024.

[20] W. Abou Saoud, A.A. Assadi, M. Guiza, A. Bouzaza, W. Aboussaoud, I. Soutrel, A. Ouederni, D. Wolbert, S. Rtimi, Abatement of ammonia and butyraldehyde under non-thermal plasma and photocatalysis: Oxidation processes for the removal of mixture pollutants at pilot scale, Chemical Engineering Journal. 344 (2018) 165–172. https://doi.org/10.1016/J.CEJ.2018.03.068.

[21] S. Saqlain, B.J. Cha, S.Y. Kim, J.Y. Sung, M.C. Choi, H.O. Seo, Y.D. Kim, Impact of humidity on the removal of volatile organic compounds over Fe loaded TiO2 under visible light irradiation: Insight into photocatalysis mechanism by operando DRIFTS, Mater Today Commun. 26 (2021) 102119. https://doi.org/10.1016/j.mtcomm.2021.102119.

[22] A.H. Mamaghani, F. Haghighat, C.S. Lee, Gas phase adsorption of volatile organic compounds onto titanium dioxide photocatalysts, Chemical Engineering Journal. 337 (2018) 60–73. https://doi.org/10.1016/j.cej.2017.12.082.

[23] A.H. Mamaghani, F. Haghighat, C.S. Lee, Photocatalytic degradation of VOCs on various commercial titanium dioxides: Impact of operating parameters on removal efficiency and by-products generation, Build Environ. 138 (2018) 275–282. https://doi.org/10.1016/j.buildenv.2018.05.002.

[24] O. Debono, V. Gaudion, N. Redon, N. Locoge, F. Thevenet, Photocatalytic treatment of VOC industrial emissions: IPA removal using a sensor-instrumented reactor, Chemical Engineering Journal. 353 (2018) 394–409. https://doi.org/10.1016/j.cej.2018.07.151.

[25] J. Li, R. Chen, W. Cui, X. Dong, H. Wang, K.H. Kim, Y. Chu, J. Sheng, Y. Sun, F. Dong, Synergistic Photocatalytic Decomposition of a Volatile Organic Compound Mixture: High Efficiency, Reaction Mechanism, and Long-Term Stability, ACS Catal. 10 (2020) 7230–7239. https://doi.org/10.1021/acscatal.0c00693.

[26] M. Kask, J. Bolobajev, M. Krichevskaya, Gas-phase photocatalytic degradation of acetone and toluene, and their mixture in the presence of ozone in continuous multi-section reactor as possible air post-treatment for exhaust from pulsed corona discharge, Chemical Engineering Journal. 399 (2020) 125815. https://doi.org/10.1016/j.cej.2020.125815.

[27] A.A. Azzaz, S. Jellali, N.B.H. Hamed, A. El Jery, L. Khezami, A.A. Assadi, A. Amrane, Photocatalytic treatment of wastewater containing simultaneous organic and inorganic pollution: Competition and operating parameters effects, Catalysts. 11 (2021). https://doi.org/10.3390/catal11070855.

[28] A.A. Azzaz, A.A. Assadi, S. Jellali, A. Bouzaza, D. Wolbert, S. Rtimi, L. Bousselmi, Discoloration of simulated textile effluent in continuous photoreactor using immobilized titanium dioxide : Effect of zinc and sodium chloride, J Photochem Photobiol A Chem. 358 (2018) 111–120. https://doi.org/10.1016/j.jphotochem.2018.01.032.

[29] A.H. Mamaghani, F. Haghighat, C.S. Lee, Systematic variation of preparation time, temperature, and pressure in hydrothermal synthesis of macro-/mesoporous TiO2 for photocatalytic air treatment, J Photochem Photobiol A Chem. 378 (2019) 156–170. https://doi.org/10.1016/J.JPHOTOCHEM.2019.04.022.

[30] J. Liu, M. Xia, R. Chen, X. Zhu, Q. Liao, D. Ye, B. Zhang, W. Zhang, Y. Yu, A membrane-less visible-light responsive micro photocatalytic fuel cell with the laterally-arranged

CdS/ZnS-TiO2 photoanode and air-breathing CuO photocathode for simultaneous wastewater treatment and electricity generation, Sep Purif Technol. 229 (2019) 115821. https://doi.org/10.1016/J.SEPPUR.2019.115821.

[31] T. Tian, L. Zheng, X. Chen, J. Xing, M. Podlogar, X. Ruan, S. Bernik, G. Li, Effect of annealing in air on the microstructural and thermoelectric characteristics of ZnO-based ceramics synthesized in a reducing atmosphere, Journal of Materials Research and Technology. 22 (2023) 348–354. https://doi.org/10.1016/J.JMRT.2022.11.091.

[32] A. Ahmad, N. Iqbal, T. Noor, A. Hassan, U.A. Khan, A. Wahab, M.A. Raza, S. Ashraf, Cu-doped zeolite imidazole framework (ZIF-8) for effective electrocatalytic CO2reduction, Journal of CO2 Utilization. 48 (2021). https://doi.org/10.1016/J.JCOU.2021.101523.

[33] Y.B. Huang, J. Liang, X.S. Wang, R. Cao, Multifunctional metal–organic framework catalysts: synergistic catalysis and tandem reactions, Chem Soc Rev. 46 (2017) 126–157. https://doi.org/10.1039/C6CS00250A.

[34] C.H. Ao, S.C. Lee, Indoor air purification by photocatalyst TiO2 immobilized on an activated carbon filter installed in an air cleaner, Chem Eng Sci. 60 (2005) 103–109. https://doi.org/10.1016/J.CES.2004.01.073.

[35] Z. Ye, Z. Ye, A. Nikiforov, J. Chen, W. Zhou, J. Chen, G. Wang, Y. Zhang, Influence of mixed-phase TiO2 on the activity of adsorption-plasma photocatalysis for total oxidation of toluene, Chemical Engineering Journal. 407 (2021) 126280. https://doi.org/10.1016/j.cej.2020.126280.

[36] J. Karuppiah, E. Linga Reddy, P. Manoj Kumar Reddy, B. Ramaraju, C. Subrahmanyam, Catalytic nonthermal plasma reactor for the abatement of low concentrations of benzene, International Journal of Environmental Science and Technology. 11 (2014) 311–318. https://doi.org/10.1007/s13762-013-0218-z.

[37] A.A. Assadi, A. Bouzaza, M. Lemasle, D. Wolbert, Removal of trimethylamine and isovaleric acid from gas streams in a continuous flow surface discharge plasma reactor, Chemical Engineering Research and Design. (2014) 1–12. https://doi.org/10.1016/j.cherd.2014.04.026.

[38] W. Abou Saoud, A.A. Assadi, M. Guiza, A. Bouzaza, W. Aboussaoud, I. Soutrel, A. Ouederni, D. Wolbert, S. Rtimi, Abatement of ammonia and butyraldehyde under non-thermal plasma and photocatalysis: Oxidation processes for the removal of mixture pollutants at pilot scale, Chemical Engineering Journal. 344 (2018) 165–172. https://doi.org/10.1016/J.CEJ.2018.03.068.

[39] W.J. Liang, H.P. Fang, J. Li, F. Zheng, J.X. Li, Y.Q. Jin, Performance of non-thermal DBD plasma reactor during the removal of hydrogen sulfide, J Electrostat. 69 (2011) 206–213. https://doi.org/10.1016/j.elstat.2011.03.011.

[40] H. Ma, P. Chen, M. Zhang, X. Lin, R. Ruan, Study of SO2 Removal Using Non-thermal Plasma Induced by Dielectric Barrier Discharge (DBD), Plasma Chemistry and Plasma Processing. 22 (2002) 239–254. https://doi.org/10.1023/A:1014895409454.

[41] L.A.S. Saldanha, N.T. das G. Santos, E. Tomaz, Photocatalytic ethylbenzene degradation associated with ozone (TiO2/UV/O3) under different percentages of catalytic coating area: Evaluation of process parameters, Sep Purif Technol. 263 (2021) 118344. https://doi.org/10.1016/j.seppur.2021.118344.

[42] A.A. Assadi, A. Bouzaza, M. Lemasle, D. Wolbert, Acceleration of Trimethylamine Removal Process Under Synergistic Effect of Photocatalytic Oxidation and Surface Discharge Plasma Reactor, 93 (2015) 1239–1246. https://doi.org/10.1002/cjce.22211.

[43] J. Palau, A.A. Assadi, J.M. Penya-Roja, A. Bouzaza, D. Wolbert, V. Martínez-Soria, Isovaleraldehyde degradation using UV photocatalytic and dielectric barrier discharge reactors, and their combinations, J Photochem Photobiol A Chem. 299 (2015) 110–117. https://doi.org/10.1016/j.jphotochem.2014.11.013.

[44] X. Feng, H. Liu, C. He, Z. Shen, T. Wang, Synergistic effects and mechanism of a non-thermal plasma catalysis system in volatile organic compound removal: A review, Catal Sci Technol. 8 (2018) 936–954. https://doi.org/10.1039/c7cy01934c.

[45] Y. Zhang, Y. Zhu, S. Tao, Z. Zhang, M. Chen, Z. Jiang, W. Shangguan, Plasma-coupled catalysis in VOCs removal and CO2 conversion: Efficiency enhancement and synergistic mechanism, Catal Commun. 172 (2022) 106535. https://doi.org/10.1016/J.CATCOM.2022.106535.

[46] A. Maciuca, C. Batiot-Dupeyrat, J.M. Tatibouët, Synergetic effect by coupling photocatalysis with plasma for low VOCs concentration removal from air, Appl Catal B. 125 (2012) 432–438. https://doi.org/10.1016/j.apcatb.2012.06.012.

[47] G. Maxime, A. Aymen Amine, B. Abdelkrim, W. Dominique, Removal of gas-phase ammonia and hydrogen sulfide using photocatalysis, nonthermal plasma, and combined plasma and photocatalysis at pilot scale, Environmental Science and Pollution Research. 21 (2014) 13127–13137. https://doi.org/10.1007/s11356-014-3244-6.

[48] A.A. Assadi, A. Bouzaza, I. Soutrel, P. Petit, K. Medimagh, D. Wolbert, A study of pollution removal in exhaust gases from animal quartering centers by combining photocatalysis with surface discharge plasma: From pilot to industrial scale, Chemical Engineering and Processing: Process Intensification. 111 (2017) 1–6. https://doi.org/10.1016/j.cep.2016.10.001.

[49] W. Abou Saoud, A.A. Assadi, A. Kane, A.V. Jung, P. Le Cann, A. Gerard, F. Bazantay, A. Bouzaza, D. Wolbert, Integrated process for the removal of indoor VOCs from food industry manufacturing: Elimination of Butane-2,3-dione and Heptan-2-one by cold plasma-photocatalysis combination, J Photochem Photobiol A Chem. 386 (2020) 112071. https://doi.org/10.1016/j.jphotochem.2019.112071.

[50] W. Abou Saoud, A.A. Assadi, A. Kane, A.V. Jung, P. Le Cann, A. Gerard, F. Bazantay, A. Bouzaza, D. Wolbert, Integrated process for the removal of indoor VOCs from food industry manufacturing: Elimination of Butane-2,3-dione and Heptan-2-one by cold plasma-photocatalysis combination, J Photochem Photobiol A Chem. 386 (2020) 112071. https://doi.org/10.1016/j.jphotochem.2019.112071.

[51] W. Abou Saoud, A.A. Assadi, M. Guiza, A. Bouzaza, W. Aboussaoud, A. Ouederni, I. Soutrel, D. Wolbert, S. Rtimi, Study of synergetic effect, catalytic poisoning and regeneration using dielectric barrier discharge and photocatalysis in a continuous reactor: Abatement of pollutants in air mixture system, Appl Catal B. 213 (2017) 53–61. https://doi.org/10.1016/j.apcatb.2017.05.012.

[52] W. Abou Saoud, A.A. Assadi, M. Guiza, A. Bouzaza, W. Aboussaoud, A. Ouederni, I. Soutrel, D. Wolbert, S. Rtimi, Study of synergetic effect, catalytic poisoning and regeneration using dielectric barrier discharge and photocatalysis in a continuous reactor: Abatement of pollutants in air mixture system, Appl Catal B. 213 (2017) 53–61. https://doi.org/10.1016/j.apcatb.2017.05.012.

[53] G. Costa, A.A. Assadi, S. Gharib-Abou Ghaida, A. Bouzaza, D. Wolbert, Study of butyraldehyde degradation and by-products formation by using a surface plasma discharge in pilot scale: Process modeling and simulation of relative humidity effect, Chemical Engineering Journal. 307 (2017) 785–792. https://doi.org/10.1016/j.cej.2016.07.099.

[54] M. Abidi, A. Hajjaji, A. Bouzaza, L. Lamaa, L. Peruchon, C. Brochier, S. Rtimi, D. Wolbert, B. Bessais, A.A. Assadi, Modeling of indoor air treatment using an innovative photocatalytic luminous textile: Reactor compactness and mass transfer enhancement, Chemical Engineering Journal. 430 (2022). https://doi.org/10.1016/j.cej.2021.132636.

[55] T. Zadi, A.A. Assadi, N. Nasrallah, R. Bouallouche, P.N. Tri, A. Bouzaza, M.M. Azizi, R. Maachi, D. Wolbert, Treatment of hospital indoor air by a hybrid system of combined plasma with photocatalysis: Case of trichloromethane, Chemical Engineering Journal. 349 (2018) 276–286. https://doi.org/10.1016/J.CEJ.2018.05.073.

[56] W. Abou Saoud, A. Kane, P. Le Cann, A. Gerard, L. Lamaa, L. Peruchon, C. Brochier, A. Bouzaza, D. Wolbert, A.A. Assadi, Innovative photocatalytic reactor for the degradation of VOCs and microorganism under simulated indoor air conditions: Cu-Ag/TiO2-based optical fibers at a pilot scale, Chemical Engineering Journal. 411 (2021) 128622. https://doi.org/10.1016/j.cej.2021.128622.

[57] B.M. da Costa Filho, V.J.P. Vilar, Strategies for the intensification of photocatalytic oxidation processes towards air streams decontamination: A review, Chemical Engineering Journal. 391 (2020) 123531. https://doi.org/10.1016/j.cej.2019.123531.

[58] F. Khodadadian, M.W. de Boer, A. Poursaeidesfahani, J.R. van Ommen, A.I. Stankiewicz, R. Lakerveld, Design, characterization and model validation of a LED-based photocatalytic reactor for gas phase applications, Chemical Engineering Journal. 333 (2018) 456–466. https://doi.org/10.1016/j.cej.2017.09.108.

[59] L. Zhang, C. Moralejo, W.A. Anderson, A review of the influence of humidity on photocatalytic decomposition of gaseous pollutants on TiO2-based catalysts, Canadian Journal of Chemical Engineering. 98 (2020) 263–273. https://doi.org/10.1002/cjce.23652.

[60] E.J. Park, H.O. Seo, Y.D. Kim, Influence of humidity on the removal of volatile organic compounds using solid surfaces, Catal Today. 295 (2017) 3–13. https://doi.org/10.1016/j.cattod.2017.02.036.

[61] C.A. Santos, N.H. Phuong, M.J. Park, S.B. Kim, Y.M. Jo, Decomposition of indoor VOC pollutants using non-thermal plasma with gas recycling, Korean Journal of Chemical Engineering. 37 (2020) 120–129. https://doi.org/10.1007/s11814-019-0406-8.

[62] M.F. Mustafa, X. Fu, Y. Liu, Y. Abbas, H. Wang, W. Lu, Volatile organic compounds (VOCs) removal in non-thermal plasma double dielectric barrier discharge reactor, J Hazard Mater. 347 (2018) 317–324. https://doi.org/10.1016/j.jhazmat.2018.01.021.

[63] A.A. Adelodun, Influence of Operation Conditions on the Performance of Non-thermal Plasma Technology for VOC Pollution Control, Journal of Industrial and Engineering Chemistry. 92 (2020) 41–55. https://doi.org/10.1016/j.jiec.2020.08.026.

[64] S. Li, X. Dang, X. Yu, G. Abbas, Q. Zhang, L. Cao, The application of dielectric barrier discharge non-thermal plasma in VOCs abatement: A review, Chemical Engineering Journal. 388 (2020) 124275. https://doi.org/10.1016/j.cej.2020.124275.

[65] Z. Jia, M. Ben Amar, D. Yang, O. Brinza, A. Kanaev, X. Duten, A. Vega-González, Plasma catalysis application of gold nanoparticles for acetaldehyde decomposition, Chemical Engineering Journal. 347 (2018) 913–922. https://doi.org/10.1016/j.cej.2018.04.106.

[66] U.H. Dahiru, F. Saleem, K. Zhang, A.P. Harvey, Removal of cyclohexane as a toxic pollutant from air using a non-thermal plasma: Influence of different parameters, J Environ Chem Eng. 9 (2021) 105023. https://doi.org/10.1016/j.jece.2021.105023.

[67] W.C. Chung, Y.E. Lee, M.B. Chang, Syngas production via plasma photocatalytic reforming of methane with carbon dioxide, Int J Hydrogen Energy. 44 (2019) 19153–19161. https://doi.org/10.1016/j.ijhydene.2018.01.156.

[68] H. Ye, Y. Liu, S. Chen, H. Wang, Z. Liu, Z. Wu, Synergetic effect between non-thermal plasma and photocatalytic oxidation on the degradation of gas-phase toluene: Role of ozone, Chinese Journal of Catalysis. 40 (2019) 631–637. https://doi.org/10.1016/S1872-2067(18)63185-7.

[69] A.A. Assadi, S. Loganathan, P.N. Tri, S. Gharib-Abou Ghaida, A. Bouzaza, A.N. Tuan, D. Wolbert, Pilot scale degradation of mono and multi volatile organic compounds by surface discharge plasma/TiO2 reactor: Investigation of competition and synergism, J Hazard Mater. 357 (2018) 305–313. https://doi.org/10.1016/j.jhazmat.2018.06.007.

[70] L. Khezami, P. Nguyen-Tri, W.A. Saoud, A. Bouzaza, A. El Jery, D. Duc Nguyen, V.K. Gupta, A.A. Assadi, Recent progress in air treatment with combined

793 photocatalytic/plasma processes: A review, J Environ Manage. 299 (2021) 113588.
794 https://doi.org/10.1016/j.jenvman.2021.113588.

795 [71] W.C. Chung, I.Y. Tsao, M.B. Chang, Novel plasma photocatalysis process for syngas
796 generation via dry reforming of methane, Energy Convers Manag. 164 (2018) 417–428.
797 https://doi.org/10.1016/j.enconman.2018.03.024.

798 [72] B.M. da Costa Filho, G. V. Silva, R.A.R. Boaventura, M.M. Dias, J.C.B. Lopes, V.J.P. Vilar,
799 Ozonation and ozone-enhanced photocatalysis for VOC removal from air streams:
800 Process optimization, synergy and mechanism assessment, Science of the Total
801 Environment. 687 (2019) 1357–1368. https://doi.org/10.1016/j.scitotenv.2019.05.365.

802 [73] S. Gharib-Abou Ghaida, A.A. Assadi, G. Costa, A. Bouzaza, D. Wolbert, Association of
803 surface dielectric barrier discharge and photocatalysis in continuous reactor at pilot
804 scale: Butyraldehyde oxidation, by-products identification and ozone valorization,
805 Chemical Engineering Journal. 292 (2016) 276–283.
806 https://doi.org/10.1016/j.cej.2016.02.029.

807 [74] L. Khezami, P. Nguyen-Tri, W.A. Saoud, A. Bouzaza, A. El Jery, D. Duc Nguyen, V.K.
808 Gupta, A.A. Assadi, Recent progress in air treatment with combined
809 photocatalytic/plasma processes: A review, J Environ Manage. 299 (2021) 113588.
810 https://doi.org/10.1016/j.jenvman.2021.113588.

811

812